Chao Kang · Dave Chan · Fenghuan Su · Peng Cui

Runout and entrainment analysis of an extremely large rock avalanche—a case study of Yigong, Tibet, China

Abstract An extremely large rock avalanche occurred on April 9, 2000 at Yigong, Tibet, China. It started with an initial volume of material of 90×10^6 m³ comprising mainly of loose material lying on the channel bed. The rock avalanche travelled around 10 km in horizontal distance and formed a 2.5-km-long by 2.5-km-wide depositional fan with a final volume of approximately 300×10^6 m³. An energy-based debris flow runout model is used to simulate the movement process with a new entrainment model. The entrainment model considers both rolling and sliding motions in calculating the volume of eroded material. Entrainment calculation is governed by a second order partial differential equation which is solved using the finite difference method. During entrainment, it is considered that the total mass is changed due to basal erosion. Also the profile of the channel bed is adjusted accordingly due to erosion at the end of each calculation time step. For Yigong, the profile used in the simulation was extracted from a digital elevation model (DEM) with a resolution of 30 m × 30 m. Measurements obtained from site investigation, including deposition depth and flow height at specific location, are used to verify the model. Ground elevation-based DEM before and after the event is also used to verify the simulation results where access was difficult. It is found that the calculated runout distance and the modified deposition height agree with the field observations. Moreover, the back-calculated flow characteristics based on field observations, such as flow velocity, are also used for model verifications. The results indicate that the new entrainment model is able to capture the entrainment volume and depth, runout distance, and deposition height for this case.

Keywords Rock avalanche · Debris flow entrainment · Yigong rock avalanche · Debris runout modeling · Soil erosion

Introduction

Debris flow event and analysis

Debris flows are rapid mass movement in steep hilly terrains where earthly materials flow down in a valley or channel usually triggered by heavy rainfall. It is usually fast-moving with variable solid concentration and large runout distance. Due to its fast-moving characteristics, debris flow is one of the most hazardous and unpredictable surface process that results in many losses of lives and property damages (Schurch et al. 2011). For example, between 2004 and 2010, there were 2,327 people killed by debris flow in China out of 6,910 who were killed by natural hazards. One recent example showing the destructive power of debris flow is the Zhouqu debris flow which occurred on August 7, 2010. It caught the residents of Zhouqu by surprise since the event occurred just before midnight, killing 1,765 people and destroying more than 5,500 houses.

In order to assess the extent of damages caused by a debris flow event, numerical modeling and debris flow analysis are often carried out. There are several approaches in debris flow modeling. These include the empirical approach, the discrete approach, and the continuum approach. In the empirical approach, calculations of the volume, speed, runout distance, and the extent of a debris flow are based on the historical observations of a large number of events; see Fannin et al. (2012) and Moffat et al. (2011). In the second approach using the discrete method, debris flow is modeled using many small elements that interact with each other (Cundall and Strack 1979). The third approach is based on continuum models in which the body of the debris is considered to be a continuum. The formulation of the model is based on physical laws such as Newton's law of motion, the law of the conservation of mass, and the law of the conservation of energy. The equations governing the motion of the debris are derived to calculate the flow characteristics, such as velocity, depth, runout distance, etc.; see Wang et al. (2010). Numerical techniques, such as the finite element method, finite different method, or the block continuum method, are often used to provide the numerical solution for the debris flow analysis. Due to the complexity of rheology of debris material and the size of a typical debris flow, it is still not possible to adopt a discrete approach which requires large computation of resources. The continuum model is a more practical approach to obtain solutions for realistic debris flow problems.

Debris flow runout simulation

In continuum modeling, there are two approaches in formulating the equations for debris flow runout analysis. The governing equations can be derived by applying the law of conservation of momentum in numerical analysis or it can be derived based on the law of conservation of energy. The first approach has been commonly used such as the dynamic analysis model (DAN) developed by Hungr (1995). DAN has been widely used in debris flow runout simulation. DAN is based on an explicit solution of the Saint Venant equations incorporating a variety of constitutive relationships in describing debris flow characteristics.

The energy model adopts the law of conservation of energy which also considers internal energy dissipation during the movement of the debris flow. As a slice-based model, the energy model determines the motion of each slice considering energy conservation in the Lagrangian framework (Wang 2008). Lateral pressure and basal resistance on individual slices are determined using the Rankine and Mohr–Coulomb theories. The momentum equations for the overall sliding mass are not examined during the calculation.

Debris entrainment and basal erosion

During the moving process of debris flow, material from the channel boundary is often eroded and mixed with the main body of the debris and becomes part of the flowing debris (Iverson 2012). This process of increasing the mass by eroding the material from the channel is called entrainment. There are various models in calculating the amount and rate of entrainment in debris flow analysis. There are basically two approaches in calculating
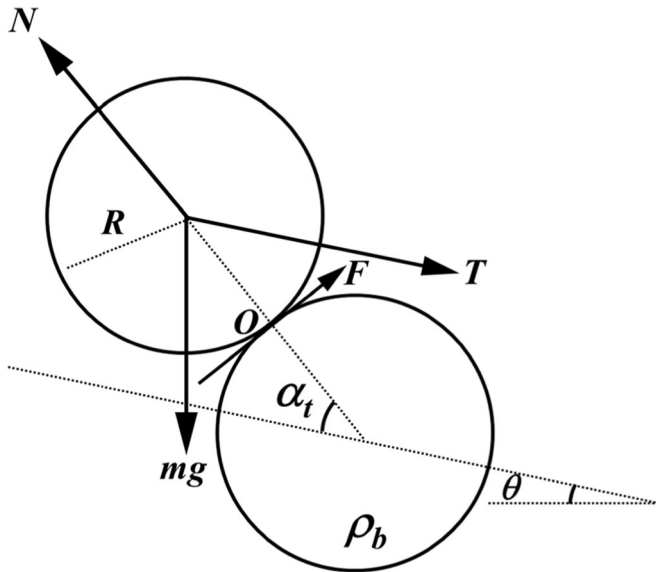
Fig. 1 Free body diagram of particle when rolling occurs

entrainment: the static approach and the dynamic approach. In the static approach, static shear stresses are calculated beneath the channel bed under the debris and failure is considered when the static shear stress exceeds the shear strength of the material (Medina et al. 2008a). The depth in which failure occurs is determined and the amount of material is calculated which will be added to the main body of the debris. In the dynamic approach, the rate of entrainment is calculated based on the rate of erosion of the material at the channel bed. The rate of erosion is determined based on the shear failure at the surface and the material is removed from the surface based on the velocity of flow of the main body of the debris (Medina et al. 2008a). It is assumed in this approach that the velocity of newly eroded material is the same as the average velocity of the debris. However, field observations indicate that the velocity of the newly eroded material is not the same as the debris (Fraccarollo and Capart 2002; Medina et al. 2008b).

Egashira et al. (2001) proposed a formula to calculate erosion rate assuming that the slope of the channel bed is always adjusted to the angle corresponding to limiting equilibrium conditions. The material in the channel left behind by an unsaturated debris will approach the limiting equilibrium slope angle. Geometrical relationship between the initial bed slope and equilibrium slope angle is incorporated into mass conservation law of eroded material to obtain the entrainment rate.

The entrainment model proposed by van Asch et al. in 2004 (Luna et al. 2012) is a dynamic 1D debris flow model that takes into account the entrainment concept based on the generation of excess pore water pressure under undrained loading on the in situ material. Flow is treated as laminar, single phase and as an incompressible continuum process. Due to the moving mass flowing on top of the erodible bed, a loading on the bed deposits is generated. The model calculates this applied load on the in situ soil through
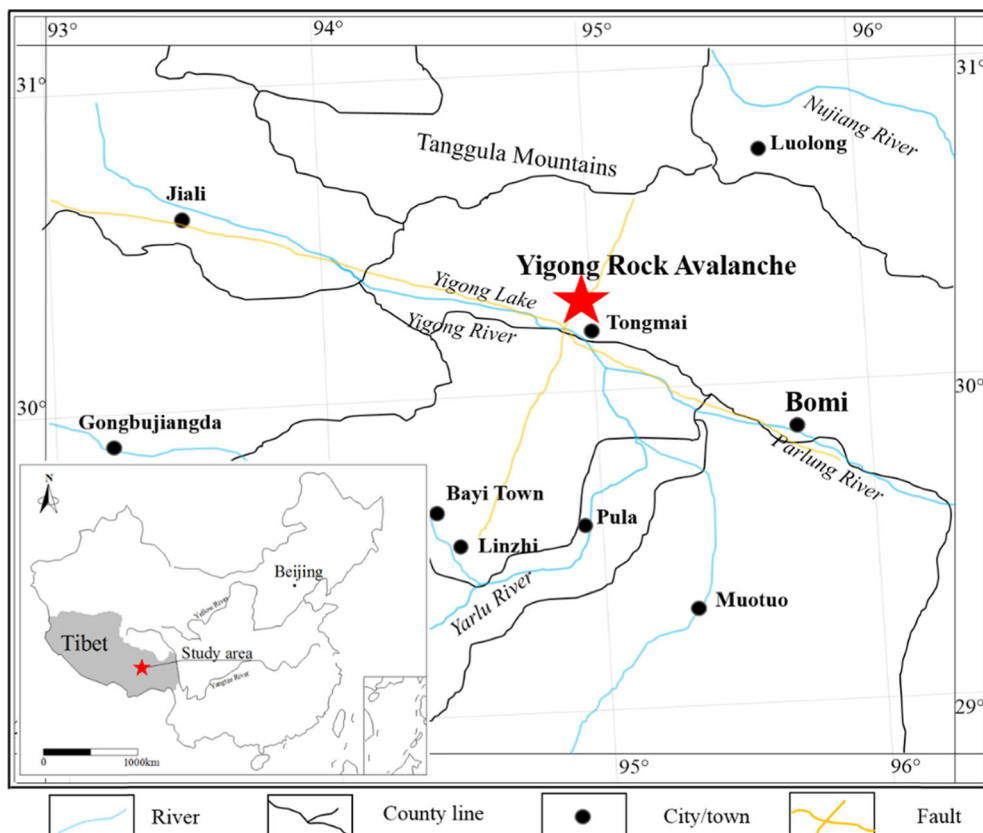

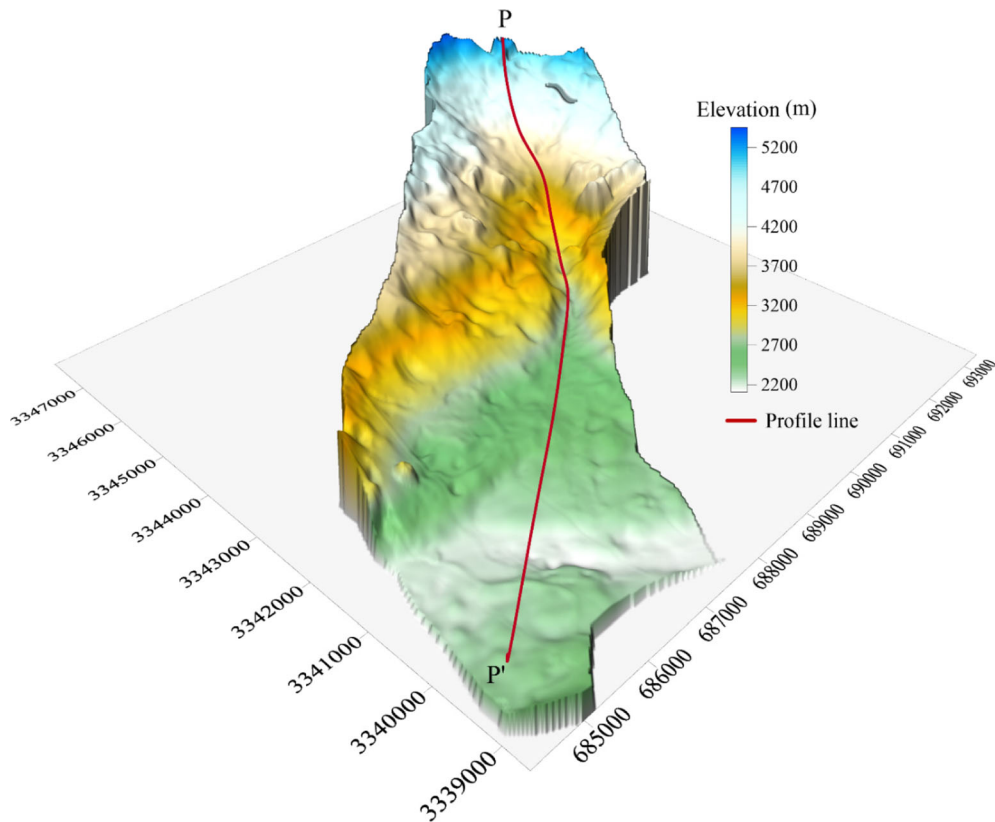**Fig. 2** Geographical location of Yigong rock avalanche

Fig. 3 Digital elevation model of Yigong rock avalanche

changes in the vertical normal stress and shear strength caused by the debris flow. The increase in pore water pressure is calculated based on the Skempton's (1954) equation. The entrainment depth is approximated using the relationship between the factor of safety at the bottom and top of soil in the channel. The model proposed by van Asch is similar to the depth-integrated model except that it considers the factor of safety for the erodible layers. Although the interaction between the debris and the channel soil is considered here, entrainment rate is not taken into account. Besides, the effect of grain size is not considered in the entrainment process, which is important, and it was illustrated by the experiments carried out by Egshira (2001).

Iverson (2012) considered the behavior of a slide block descending an erodible slope with the ability of incorporating soil on the static bed. Newton's second law was first applied on the sliding material. Then, Coulomb friction rule was applied and basal friction resistance calculation was improved by taking the shear rate into account. The frictional resistance consists of a constant component of friction resistance and a velocity-dependent component. After considering the rate-dependent friction, entrainment rate based on the change in weight of the sliding block was obtained.

De Blasio et al. (2011) suggested a semi-empirical model to calculate entrainment. In the semi-empirical model, entrainment rate depends solely on the tangential component of weight at the base of the flow and on the average velocity of the debris flow. Critical shear stress is used as the thereshold to determine the occurance of entrainment. Data from Fjæland

debris flow used for dynamic quantities and for erosion effects is utilized to calibrate the model. This model seems promising
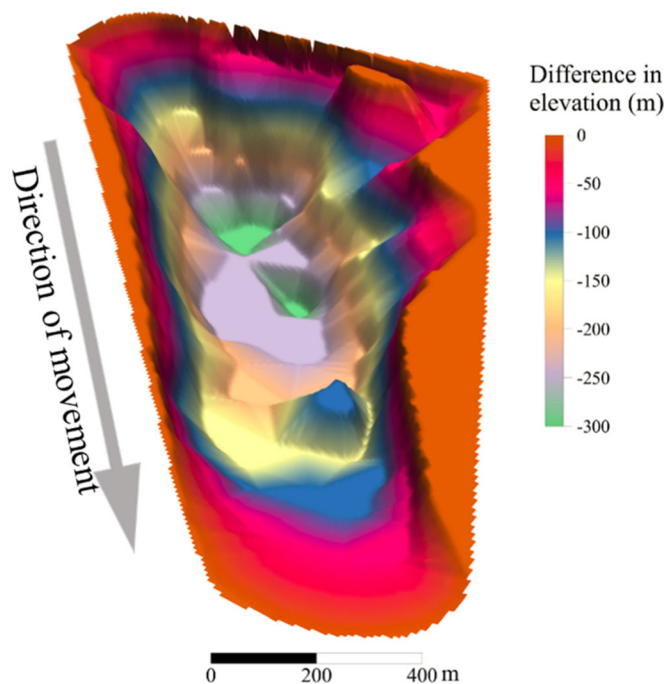

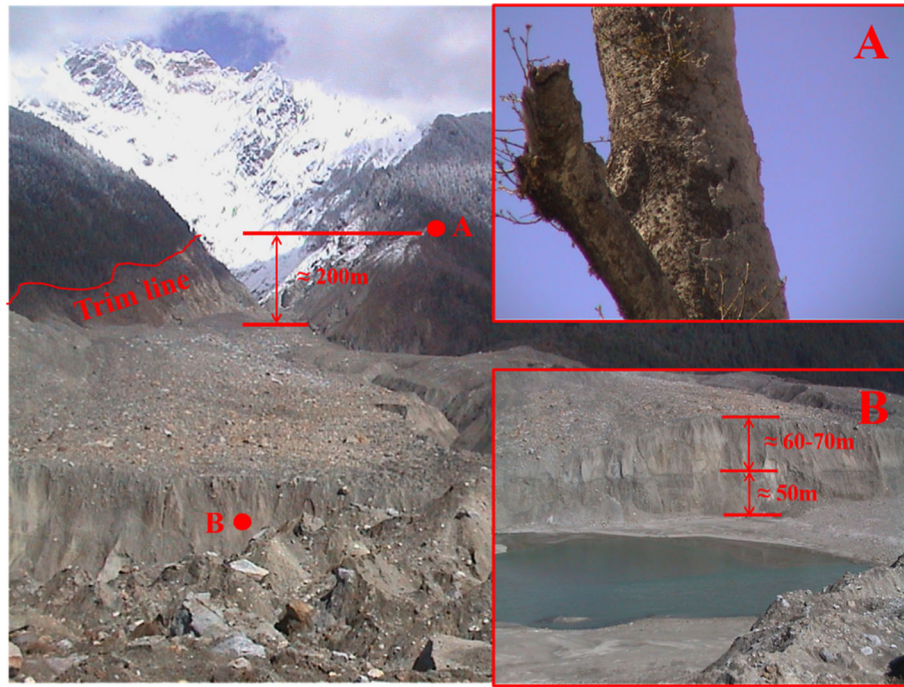**Fig. 4** Variation of elevation at source area of YRA (revised from Wang (2006))

Fig. 5 Evidence of flow height near the outlet of Zamu Creek (photo by Chen 2015)

since it relates debris flow velocity and basal shear stress to entrainment.

After comparing the pros and cons and the limitations of those models, a new progressively scouring model was developed. In applying the model to solve practical problems, the model was used to calculate the debris flow characteristics and entrainment at Yigong. The calculated flow characteristics such as debris flow height, entrainment depth, and thickness of debris deposition are compared with field observations.
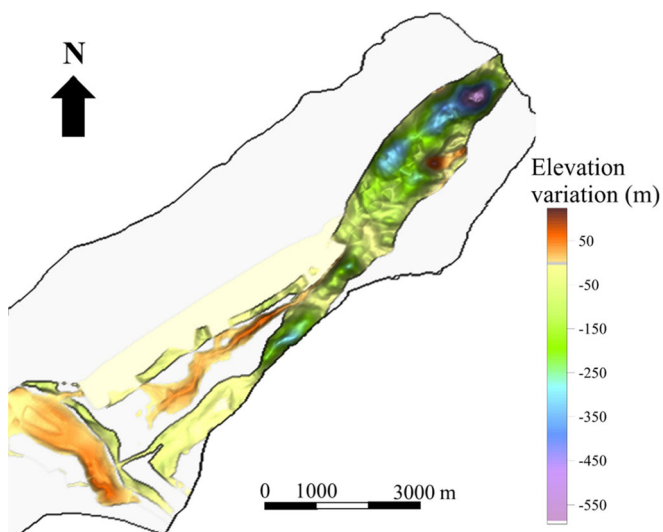
Runout model and the new entrainment model

Runout model
As described earlier, two approaches have been applied to simulate debris flow runout process. Since the energy model considers the internal energy dissipation during mobilization, motion, and deposition, it is employed to incorporate the new entrainment model.

In the slice-based model, the energy model determines the motion of each slice based on the energy conservation equations using the Lagrangian difference scheme (Wang et al. 2008). The change in kinetic energy of a sliding mass consists of changes in potential

Fig. 6 Elevation variation obtained by subtracting DEM after event from the before event

Fig. 7 Observed largest particle embedded into deposition fan (photograph by Chen 2015)

energy, work done by resistance forces along the base of the sliding mass, and work due to internal deformation of the debris. Lateral pressure and basal resistance on individual slices can be calculated using the Rankine and Mohr–Coulomb equations. Longitudinal spreading is mainly due to velocity gradient ($\partial u/\partial x$) that results from a combination of forces acting on the debris which include lateral earth pressure, gravitational force, and shearing resistance. The governing equation of the runout model is:

$$\frac{d}{dt}\left(\frac{1}{2}m\overline{u}^2\right) = mg\overline{u}\sin\theta + \frac{1}{2}mgh\,\overline{e}_{zz}$$
$$+ P_L\overline{u}_L\cos\theta_L - P_R\overline{u}_R\cos\theta_R - T\overline{u} - \int_V \tau_{ij}e_{ij}\,dV \tag{1}$$

where m is the mass of the slice, $\overline{u}$ is the mean velocity of the slice along the base of the slice, g is gravity acceleration, θ is the inclination of the base of the slice with respect to the horizontal, P_L and P_R are interslice forces exerted on the left and right sides of the slice, T is the shear force acting along the base of the slice, τ_{ij} are components of the stress tensor, and e_{ij} are components of the strain rate tensor. Detail formulation and discussion of the model can be found in Wang et al. (2010) and Wang (2008).

The new entrainment model

In static approach of entrainment calculation, static equilibrium is considered between the flow frictional forces, τ_b, and the basal resistance forces, τ_{res}, in each computational time step (Medina et al. 2008a). If equilibrium does not exist, the model estimates the magnitude of entrainment from:

$$\tau_b + h_{ent}\rho g\sin\theta = c + |h + h_{ent}|\rho g\cos\theta\tan\phi_{bed} \tag{2}$$

where h_{ent} is the entrainment depth, θ is slope angle, c is the cohesion, h is flow height, ρ is the bulk density of the debris, and ϕ_{bed} is the bulk friction angle of the bed material.

In dynamic approach, same failure mode is considered as that in static approach except that Newton's second law is applied on the erodible material. So, the amount of entrained material depends on the availability of momentum (Medina et al. 2008b), given by

$$\frac{\partial z}{\partial t} = \frac{(\tau_b - \tau_{res})}{\rho V} \tag{3}$$

where $\partial z/\partial t$ is the rate of entrainment and V is the mean velocity of the flow.

In the new entrainment model, it is considered that granular particles lying on the channel bed is eroded progressively. Granular particles are modeled using uniform size sphere (disk in the case of 2D analysis). Particles are mobilized due to shear stress exerting on the particles. According to the analysis (Cheng et al. 2003; Shodja et al. 2003), normally initiation drag force for the rolling action is less than that required for basal shear failure. Therefore, it is reasonable to assume that rolling motion is the dominant motion in the initial stage of entrainment. However, both rolling motion and sliding motion are considered in the formulation of the entrainment model.

Based on the experiments from Fraccarollo and Capart (2002), it is obvious that the vectors representing the velocity of flow "particles" are almost parallel to the channel bed. Therefore, in the derivation of the equation, it is assumed that the forces acting on the particle are based on particle movement parallel to the sliding surface. Hence, the forces are assumed to be tangent to the slopes.

In calculating the drag force for the initiation of the rolling action, it is assumed that a particle will rotate around point O as shown in Fig. 1. Drag forces due to the moving debris above the bed are assumed to apply at the center of the particles. It is assumed that the particle will rotate around the contact point with the adjacent particle located downstream. Newton's law of motion
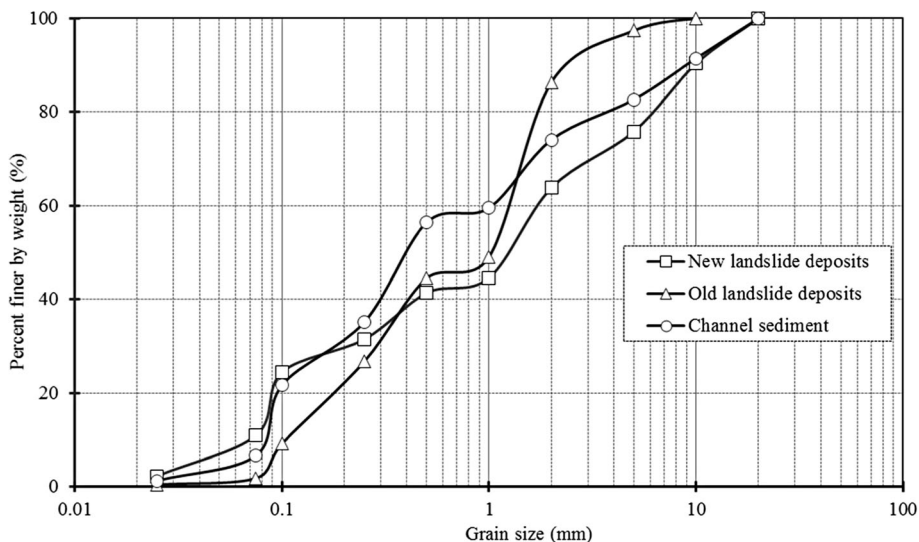

Fig. 8 Grain size distributions of fine particles ($d < 400$ mm) sampled from runout path of YRA (test carried out by Zhou 2015)
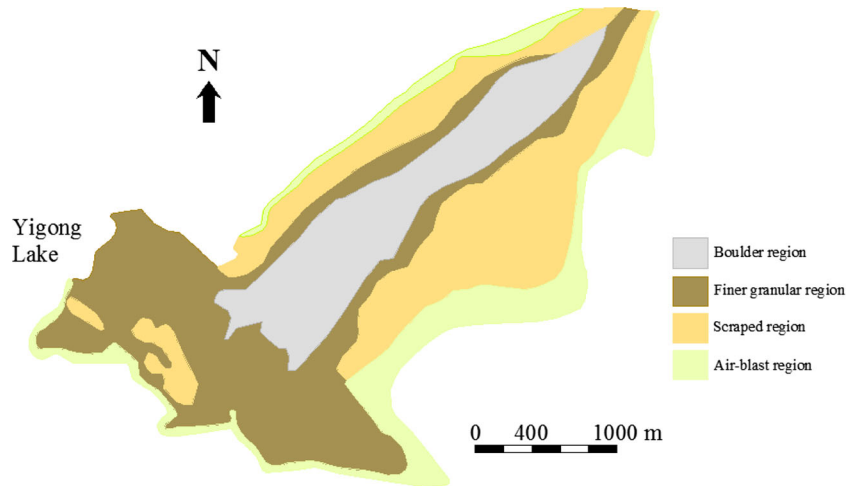
Fig. 9 Zoning map of deposition fan of YRA (Zhang and Yin 2013)

is applied to calculate the acceleration, velocity, and displacement of the particle. The moment equation is given by

$$\frac{TR}{(I + mR^2)} sin\alpha_t - \frac{mgR}{(I + mR^2)} \cos(\alpha_t + \theta) = \frac{\partial^2 \alpha_t}{\partial t^2} \quad (4)$$

where T is the drag force required to initiate particle rolling, R is the radius of the rolling particles (d_{50} is adopted here), I is moment inertial which is equal to $m(3R^2 + L^2)/12$, $L = 1$ m for 2D, m is the mass of the particle (for 2D, $m = \pi R^2 \rho_b$), ρ_b is the density of bed sediment particle, a_t is the angle between channel bed and connection line of centers of those two particles, θ is the slope angle, g is the gravity acceleration, $\partial^2 \alpha_t / \partial t^2$ is angular acceleration, and t is time.

It is also assumed in the derivation that once the particle moves over adjacent particle located downstream, it is considered to have been eroded and will be added to the total mass of the debris. Based on the equation of rolling motion (Eq. [4]), the entrainment

time, which is the time required for one particle to move from initial position to become part of the debris, can be estimated. The entrainment rate is defined as the height of the particle exposed to the flow divided by the time needed for it to be eroded. So, for different α_o, initial condition of α_t, entrainment rate, $\dot{E}_i$, is defined in Eq. [5].

$$E_i = \frac{2R sin\alpha_{oi}}{t_i} \quad (5)$$

t_i, in Eq. [5], is the time required for one particle to roll from the initial position, α_o, to the vertical position when α_t is equal to ($\pi/2 - \theta$). It is assumed in the derivation that once the particle moves to the top of the overriding particle downstream, it is considered to be part of the debris. Therefore, if shear force exerted on the particle is known and particle properties are determined, t_i can be obtained by solving Eq. [4]. When shear force exerted on the particle is larger than the friction on the particle, the entrainment mode changes from rolling motion into sliding motion.
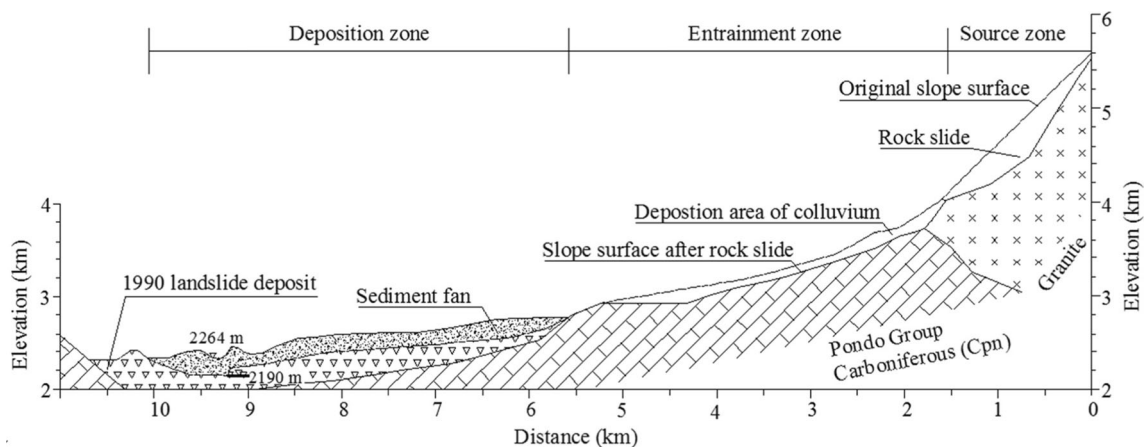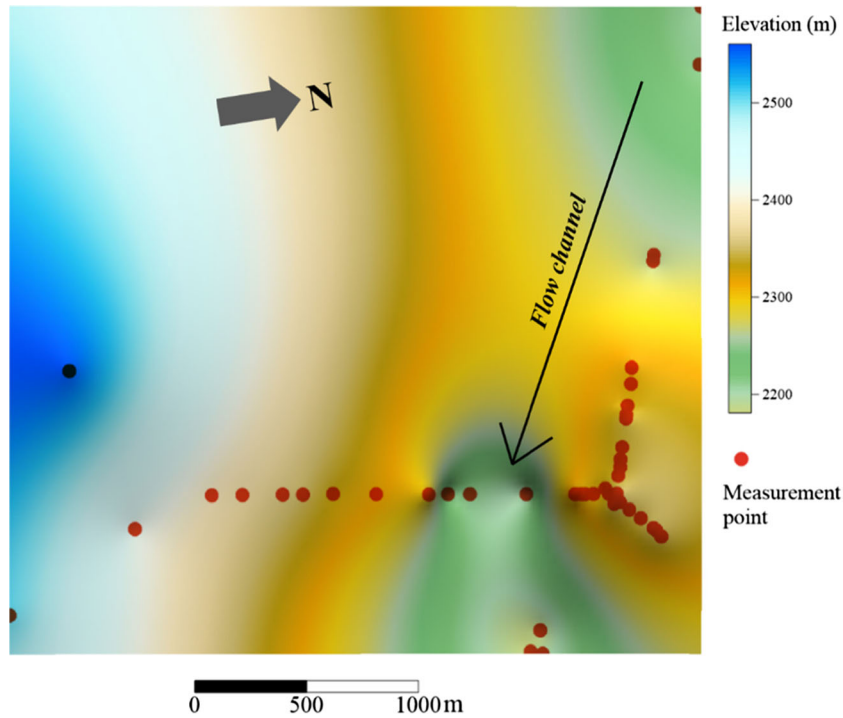

Fig. 10 Longitudinal profile along YRA path

Fig. 11 Terrain of deposition fan surveyed 2 years later

Since α_o varies from one location to another and it is not easy to be determined, a probabilistic approach is adopted and α_o is assumed to follow a probability density function (PDF) using a normal distribution. Selecting the parameters for the PDF is important in the entrainment calculation. The mean value of the normal distribution function can be estimated for a particular case (Fenton et al. 1977), but its value is site specific. The value of α_o can also be estimated from the relationship between void ratio and internal friction angle, and the relationship between particle protrusion and void ratio (Okada et al. 2007). After the PDF has been

determined and the entrainment rate for each specified α_o is known, the entrainment rate can be obtained from Eq. [6].

$$E = \sum_{i=1}^{n} \left(E_i \, P_i \right) \tag{6}$$

in which n is the number of division between 0° and 90° based on the increment of α_o.

a Pre-event (LandsatTM-5, 1998-12-15)

b Post-event (LandsatTM-7, 2000-05-20)

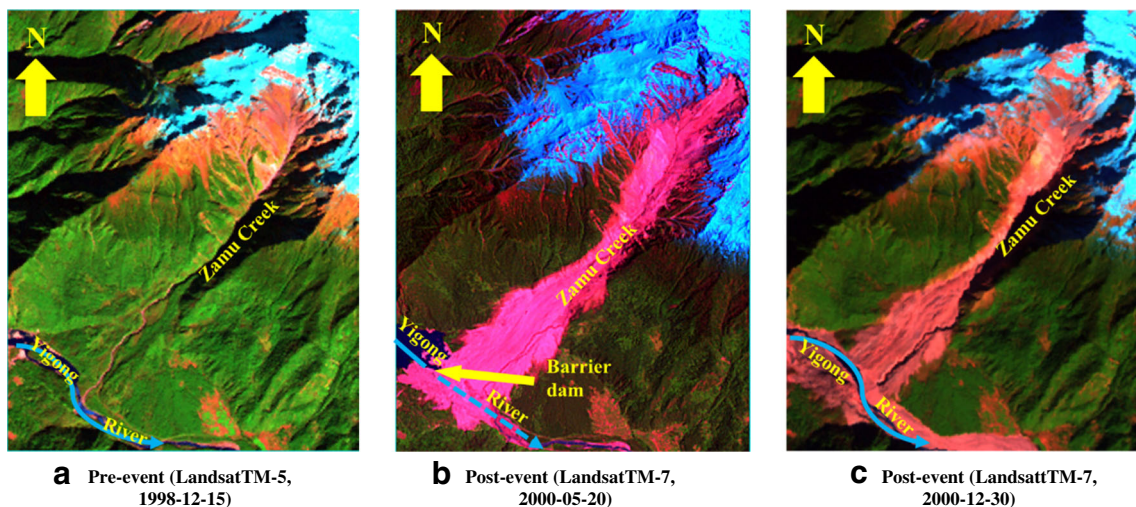**c** Post-event (LandsattTM-7, 2000-12-30)

Fig. 12 Aerial photos at different time indicated that **a** there is an old debris fan (1900), **b** the river was blocked by YRA (2000), and **c** flow channel after overtopping the dam (Wang 2006; Lv et al. 2002)
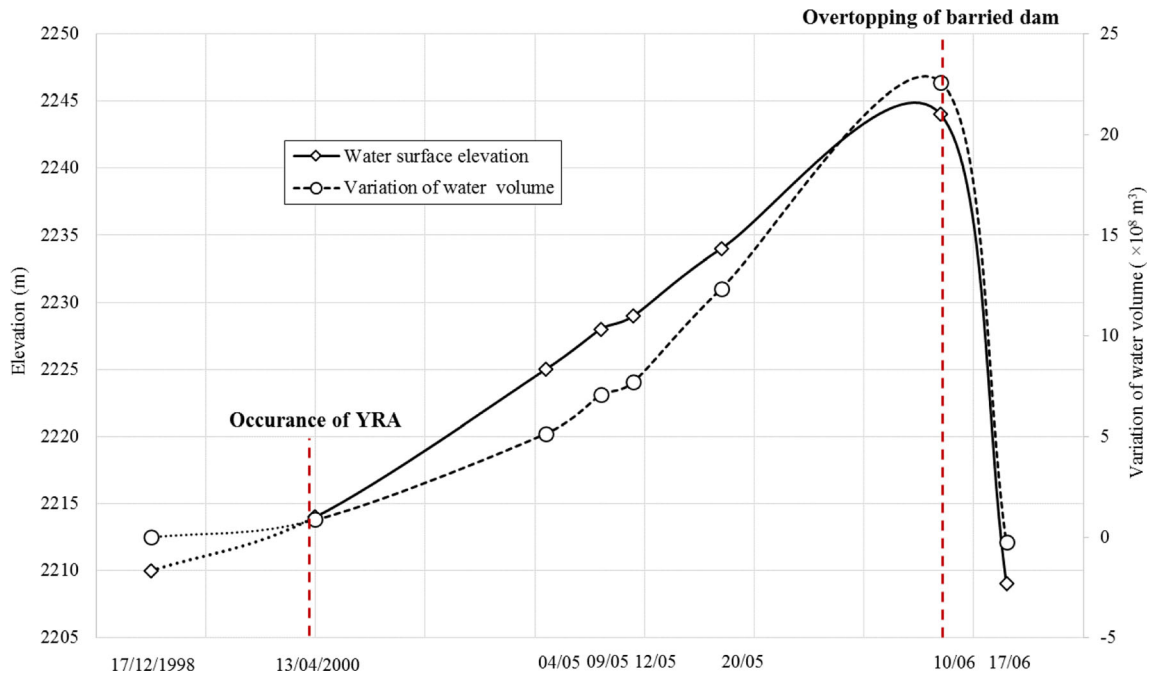
Fig. 13 Variation of Yigong lake elevation

Description of Yigong rock avalanche

Geomorphology

On April 9, 2000, a rock avalanche occurred at Yigong, Tibet, China (Fig. 2). This event is considered as one of largest non-seismic mass movement in recent years (Zhang et al. 2013). The Yigong rock avalanche (YRA) is located at N30°12′03″, E94°58′03″, Zamu Creek, a tributary of the Yigong River (Lv et al. 2002). Zamu Creek is a typical channeling valley. The slopes of its lateral mountains are between 30° and 35°. The bottom width of the creek is between 50 and 150 m (Zhang et al. 2013). The elevation at the source zone of the rock avalanche is about 5,350 m, and the elevation of the Yigong River bed is about 2,188 m (Fig. 3; Wang 2006). The runout path is plotted in Fig. 3 denoted by line P-P', which is also the profile line used in the current simulation.

Features of source area

The source area of YRA is situated at the top of the catchment area of Zamu Creek with a drainage area of 20.2 km² and a length of 7.9 km. The total bare source zone of YRA is about 12.9 km². The elevation of the source ranges from 4,000 to 5,525 m. The geometric center of the rock slide has an elevation of about 4,600 m (Xu et al. 2012). The bare rock is mainly consisted of granite, but due to two intersecting faults in this region, geological activities and physical weathering process, a wedge-shaped sliding body was formed in the source area. From the digital elevation model (DEM) before and after the occurrence of the rock avalanche, it is estimated that the source volume was around 90×10^6 m³ with 318 m in maximum depth (Fig. 4; Wang 2006). In Fig. 4, the negative number means the decrease in elevation after the rock avalanche.

Time and duration of the event

According to the seismogram of the nearest seismic station, the Linzhi seismic station, which is located 110 km southeast of the site, felt the first vibration of the ground which occurred at 19:59:42. The energy released from the tremor is equivalent to a 2.9-magnitude earthquake. After that, two consecutive 3.5-magnitude earthquakes were detected (Ren et al 2001). This coincides with the description from a local residence whose home is 10 km away from the source area of rock slide and 300 m away from the western margin of final debris deposition. The eyewitness recalled that the ground was shaking violently at around 20:00 (Xu et al. 2012). Therefore, it can be concluded that the event occurred at around 20:00 on April 9, 2000.

Since YRA occurred suddenly, there was no data collected for the elapsed time. The time deduced from recorded seismic wave indicated that this event lasted for at least 6 min (Ren et al. 2001). A farmer, who was working at Yigong Tea Farm at the time, cited that from the time he saw a cloud of thick smoke to the time he saw the debris flowed out of the Zamu Creek is around 3 min. Others have quoted that the duration of this event is around 10 min (Yin 2000a, b). Although the elapsed time varies from 3 to 10 min, it is nonetheless that this event lasted a short time.

Description of velocity, runout distance, and height during its movement

For such a rapid large rock avalanche, it is very difficult to monitor the velocity during the event since not only it occurs randomly, but
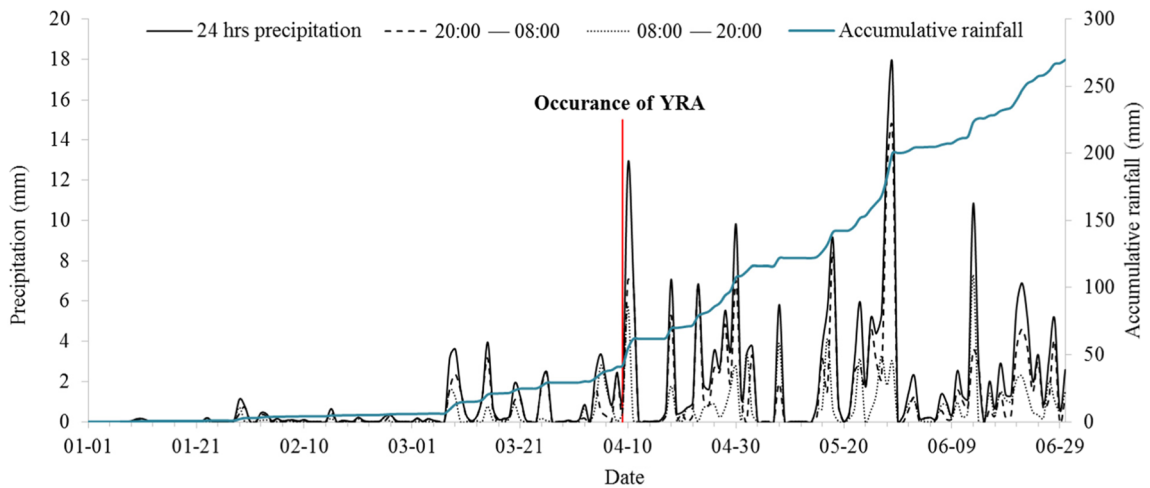
Fig. 14 Ground surface temperature and precipitation before and after the event interpolated from surrounding weather stations. **a** Weather stations located around Yigong area; **b**, **c** ground surface temperature and precipitation interpolated from the stations shown in **a**
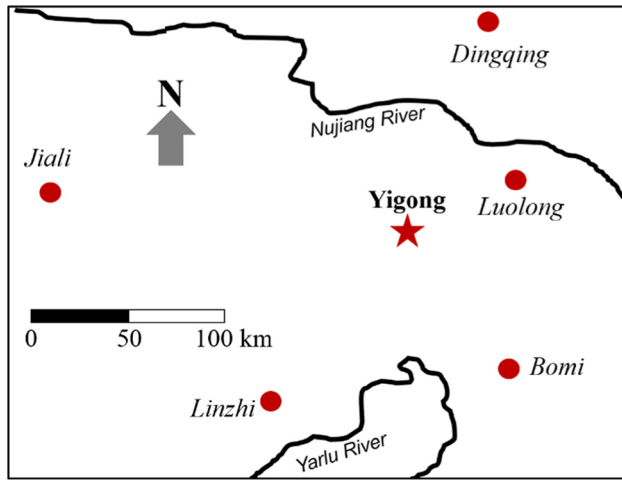
a
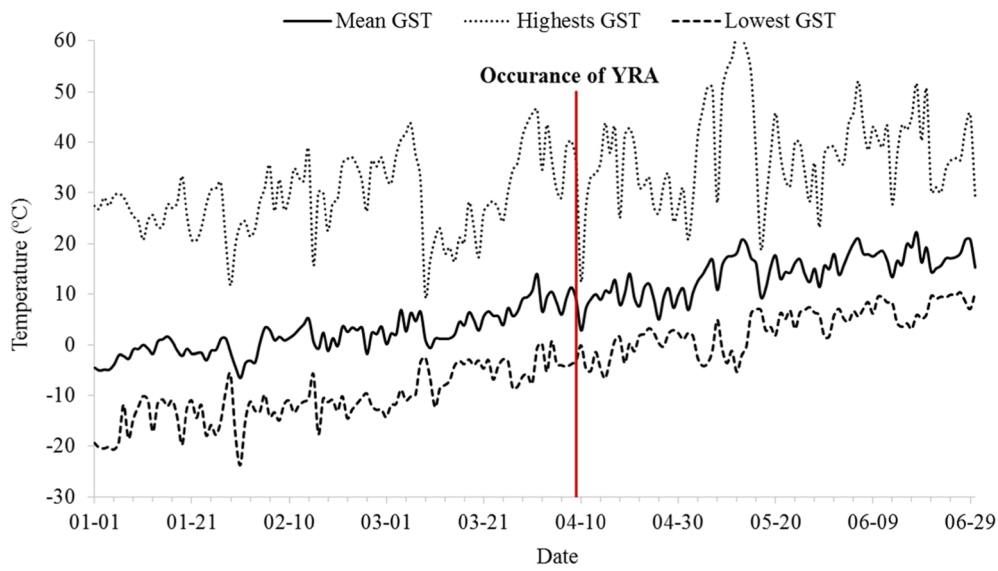
b

c

also it is difficult to install monitoring devices so that it will not be damaged. Normally, velocity is deduced from seismic surveillance data and the estimated average velocity is around 48 m/s. Local citizens who were working near the outlet of Zamulong Creek described that nine gales were felt at the outlet. Destroyed tress and charred trees along the channel also affirmed that the rock avalanche moved with a very high speed (Fig. 5).

Field investigation showed that YRA climb over the mountain near the outlet of Zamu Creek (Fig. 5). The picture taken at point A at the top right corner shows that the debris had reached that location. The photo at point B shows the cross section of deposition fan. It is obvious that the deposited material lies on top of the old debris deposition fan and the new deposition height is around 60 to 70 m. The elevation difference between the deposition and peak of mountain is about 200 m. Adding the thickness of the deposition, it is suggested that maximum flow height of YRA at that site is nearly 200 m if super elevation is not considered. YRA stopped after it reached the south bank of Yigong River. Therefore, the horizontal travel distance is around 10 km (Yin 2000a, b). This distance is estimated along the flow channel.

Description of entrainment and final deposition

During the sliding process, drag force exerted by the sliding debris could erode materials lying on the channel bed. This process could increase the volume of the final deposition and increase the velocity of moving debris. The entrainment zone in Zamu Creek is mainly composed of loose colluvial materials, distributed not only on the creek banks, but also on the channel bed. Erodible material in Zamu Creek is mainly located at an elevation between 3,000 and 4,000 m.

Deposition zone consists of boulders moved from source area and loose debris materials in the entrainment zone. In this region, particle size changes from the central area to deposition boundary. The accumulated debris at the central area in the deposition zone composes mostly of bounders having a diameter over 3 m, and the total volume of the boulders is around 30×10^3 m^3.

Elevation variation of Zamu Creek before and after YRA is shown in Fig. 6. It seems that the maximum elevation variation is around 500 m which is larger than that reported by Wang (2006). The DEM used to plot the elevation variation map is based on the survey a few months after the event. Snow melt and other topographic evolution process may introduce errors in the elevations.

As grain size in rock avalanche fan varies from very fine particle to boulders, it is very difficult to sample particles of all sizes for sieve analysis, so coarse particles which size is greater than 400 mm were excluded in sampling process. The observed largest particle is around 22 m (Fig. 7). Grain size distribution of sampled fine particles is shown in Fig. 8.

Interpretation of remote sensing images shows that the total volume of YRA is about 300 million m^3 (Wang and Lv 2001). From the aerial photo after the event, it is measured that YRA formed a 2,500-m-long and 2,500-m-wide deposition fan. Zoning map of deposition fan is shown in Fig. 9 and the longitudinal profile is shown in Fig. 10. Average depth of the deposit is 60–70 m (Yin 2000a, b).

Since small size rock avalanche frequently occurred. A discharge channel was excavated in the deposition fan in 2000. The shape of deposition fan has been changed considerably, but the main features of YRA were still visible when field investigation was conducted in 2002. The elevation of the channel bed is about 2,190 m (Yin 2000a, b). Surveyed topographic map measured using total station shows that the deposition fan has been cut down by about 100 m (Fig. 11).

Consequence of the Yigong rock avalanche

Although the YRA is an extremely large rock avalanche in the recent year; fortunately, there was no casualties reported. However a barrier dam was formed and it blocked the Yigong River (Fig. 12). The water surface elevation before this event was constant at about 2,210 m, and the total amount of water in Yigong Lake was 70×10^6 m^3. After the river was blocked, water surface level rose rapidly (Lv et al. 2002). A 30-m-deep discharge channel was completed on June 3, 2000 and the lake level started to drop on June 10, 2000; see Fig. 13, (Liu et al. 2013). It took almost 1 week for the water level in the lake to return to the river level before the event. Unfortunately, 4,000 people were stranded in this process putting their lives at risk. Besides, many villages and farmland were flooded (Yin 2000a, b).

Possible triggers and evidence of the triggering mechanism

Since two faults, an east-west Jiali right-handed strike slip fault and south-north Yigong–Lulang strike slip fault, cross Zamu Creek (Xu et al. 2012), with large temperature difference between day and night, joints and fissures are well developed at this region (Zhou et al. 2000).

Since there was no record of seismic activity before the rock avalanche, variation of temperature and rainfall become the most likely triggers of YRA. As the temperature record of one weather station cannot accurately describe the weather change of a small area few kilometers away from this station, according recorded land surface temperature at three weather stations around Yigong area, see Fig. 14a, the ground surface temperature (GST) and precipitation were interpolated using Inverse Distance Weighting Method. The interpolated results are shown in Fig. 14b, c. It is clearly shown that large differences in GST between day and night time were detected. Due to the variation of temperature, snow melts when temperature rises above zero, and water freezes if temperature drops below 0°C. This freeze–thaw process can induce to active physical weathering. In this freezing process, the force of expansion caused by freezing of water could result in the development of fissures and crack. In the thawing process, melted water can fill the pores caused by crack development. Also, the new filled water could cause the increase in pore water pressure in the cracks and the decrease in effective stress. When the shear stress exceeds the shear strength of the material, a wedge can form and it may slip suddenly from the mountain top.

Figure 14b indicates that the mean GST in this region rose from −0.6 °C to 10.7 °C 10 days before the occurrence of YRA while the highest GST increased from 9.7 °C to 46.7°. Although the mean temperature dropped to 5.9 °C 3 days before the event, it rose to around 11.4 °C 1 day before the event. On the day of the event, the highest GST was 36.0 °C. It was also recorded that the highest daily temperature of this area mostly appeared at around 16:00 to 18:00 (Zhou et al. 2000). Adding the time needed for heat conduction in rock blocks and air in open spaces between rock blocks, this may explain why this event occurred few hours late after 1800.

The interpolated daily precipitation shows that there were only 2–4 mm precipitation one day before YRA see Fig. 14b. This

Table 1 Parameters in the simulation

Run-out model parameters	Values
Unit weight (kN/m^3)	20
Internal friction angle (°)	13
Basal friction angle (°)	12
Turbulent coefficient (m/s^2)	500
Entrainment model parameters	
Particle size d_{50} (mm)	300
Standard deviation of α_o (°)	0.1
Mean value of α_o (°)	12
Particle density (kg/m^3)	2,600
Bulking factor	1.3

amount of water is not enough to reduce the strength or increase the driving force for the material at source area. If surface evaporation is taken into account, the water is lesser. Therefore, it is most likely that melted snow provides the source of water for loosely packed material lying on channel bed since the mean GST was higher than the freezing point. Therefore, it means that variation in temperature resulted in changes in snow and ice melting causing pore water pressure to increase is the main trigger for the occurrence of YRA.

Runout and entrainment analysis

According to the data collected in the field, granular particles deposited at the rock avalanche fan mainly came from the source area and transported from the entrainment zones. If the entrainment zone is close to the deposition fan and rock fragmentation has not taken place, particles located in the entrainment region should be about the same size as those in the deposition zone. Although samples can be collected in the deposition fan, it is very

difficult to conduct sieve analysis since the particle ranges from very fine (clay) to very large (boulder). Therefore, a practical way to estimate the medium size of the material is to analyze the composition of the material. According to the description of the loose material at the deposition area (Xu et al. 2012) and particle size distribution curve obtained from the laboratory test, it is estimated that the medium size, d_{50}, of the material is around 300 mm.

Since it is nearly impossible to measure α_o for all particles in place, an indirect method to estimate the mean of normal distribution is used here. The value of α_o may be obtained from the pivoting angle and the slope angle. In the simulation, the pivoting angle of the angular particle, ϕ_p, is estimated using the empirical relationship from Li and Komar (1986). The average slope angle can be obtained from the digital elevation model. A mean value of the normal distribution PDF of 12° is calculated based on the relationship $\alpha_o = (\pi/2 - \phi_p - \theta)$. Based on the results of sensitivity analyses, the standard deviation is found to be equal to 0.1 for this case. When the particles are eroded, close-packed particles mobilize and become loose. Porosity of the eroded material increases. This will cause the expansion of the material. Based on the law of conservation of mass, a bulking factor is defined as ratio between the density of the material in the channel bed and the density of the debris. In the calculation, the volume of the eroded material in the debris is equal to the volume before it is eroded times the bulking factor.

The Voellmy model is used to calculate the shear stress exerting on channel bed. Xu et al. (2012) used the friction angles ranging from 0.52° to 20° on different longitudinal sections of YRA. Since the model is developed based on dry granular flow, a lower friction angle and basal friction angle are suggested to offset the effect of water on the soil friction. An internal friction angle of 13° and basal friction angle of 12° were used in the simulation which is smaller than that used by Xu et al. (2012). A turbulent coefficient of 500 m/s^2 is adopted in the simulation which is a little bit larger than the medium value suggested for rock avalanche (Luna et al. 2012), but it is still within the
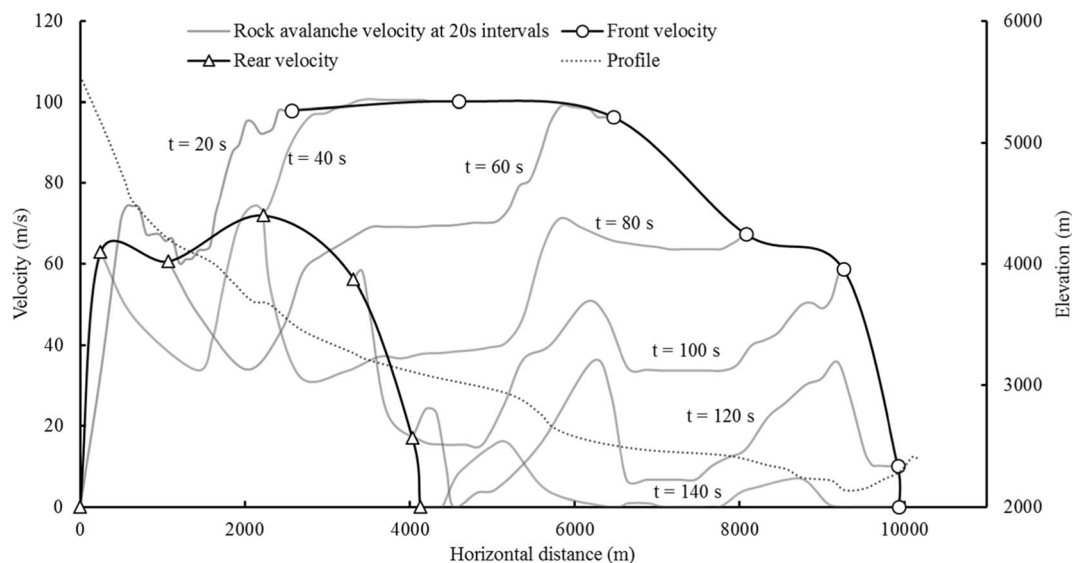

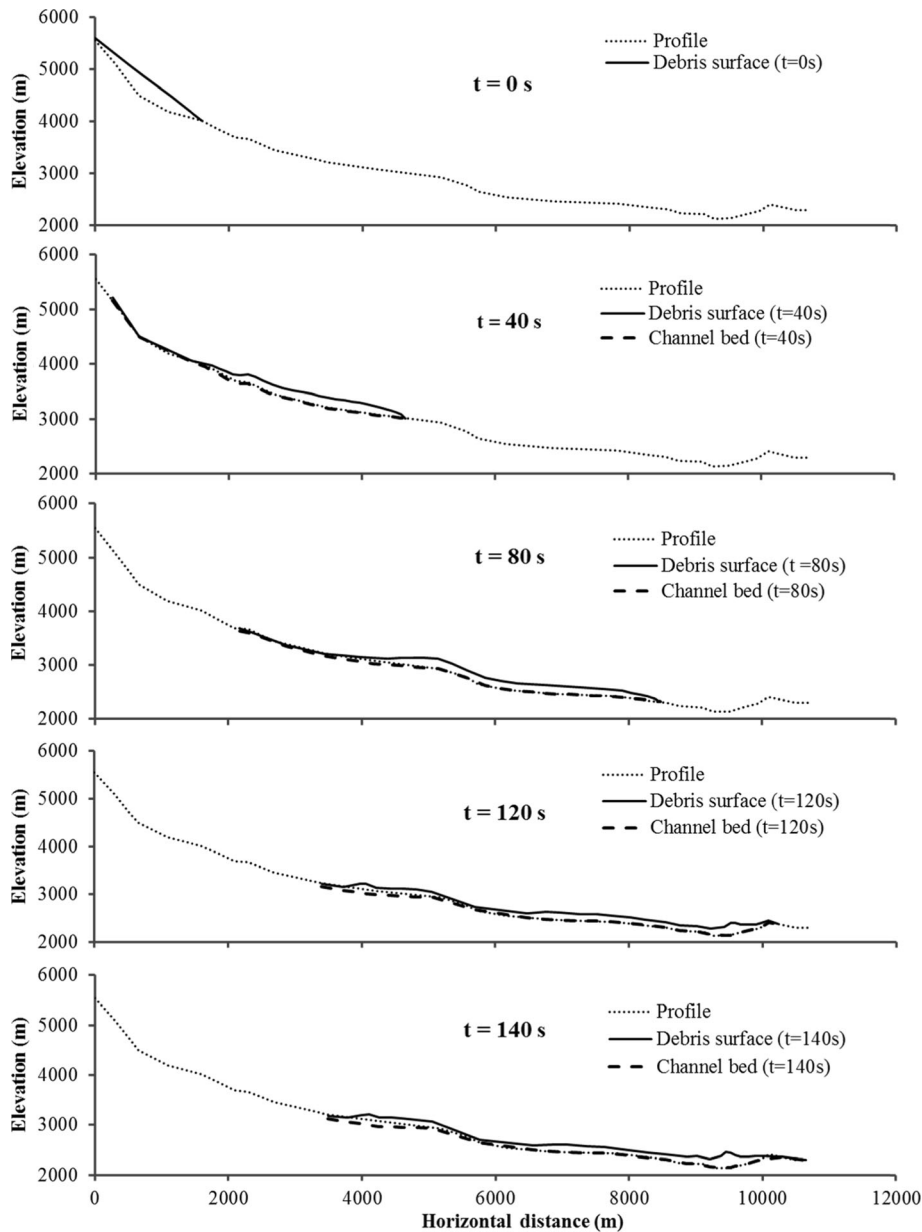**Fig. 15** Velocity and its variation in the simulation

Fig. 16 Change of profile in each simulation steps

reasonable range of values. Parameters used in the simulation are summarized in Table 1.

The longitudinal profile shown in Fig. 10 is divided into three zones from top to bottom: source zone, entrainment zone, and deposition zone. In the simulation, original slope surface changes due to the entrainment at medium part of the profile. Based on the observed source volume and area of source material in 2D, a uniform width, 173 m, is calculated which keeps constant in the simulation. The number of slices could impact the calculation results. To investigate the sensitivity of the number of slice on the model results, the source material is divided into 50 slices in another run. The difference in runout distance, velocity and total volume are 0.6, 0.1, and 1 %, respectively. After evaluating the required time for the calculation and resolution of calculated results, the model with 30 slices is adopted.

Simulation results

Results of runout and entrainment analyses
In the simulation, the front velocity of the rock avalanche was calculated. The calculated front velocity of YRA increases in the first 30 s and then gradually drops when the material reaches a relatively flat area as shown in Fig. 10. A plot of the velocity versus path distance is shown in Fig. 15. The maximum velocity occurred at a path distance around 3,500 m. At about 140 s, the front of the debris almost stopped moving but the remaining part kept moving at a very small velocity. The change of profile of YRA at different time stage is shown in Fig. 16.

Since YRA has a large initial volume travelling at high velocity, the entrainment rate is expected to be very large. The entrainment
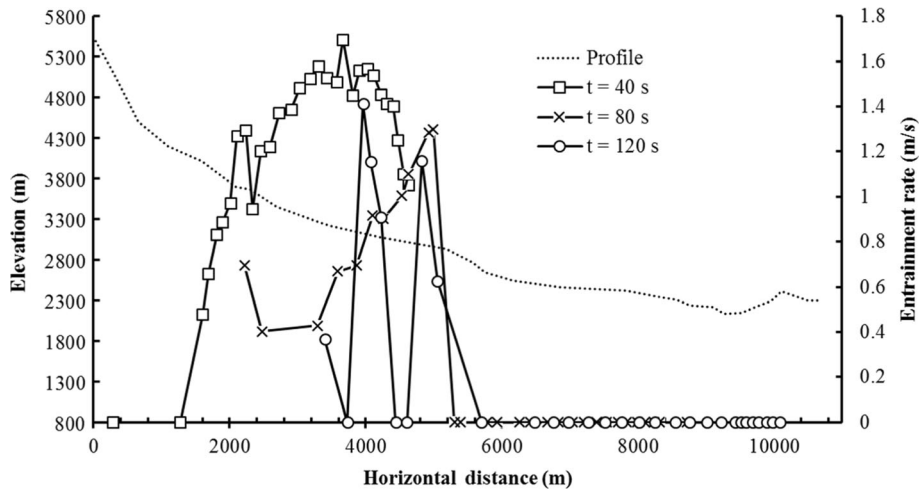
Fig. 17 Entrainment rate along the channel at different time stage

depth is assumed to be 280 m in runout analysis using DAN (Zhang 2013). The entrainment rate of each slice at different time stage in this simulation is shown in Fig. 17. The maximum entrainment rate is 1.79 m/s at the initial stage (Fig. 18). The entrainment rate increases after 100 s since the accumulated flow height has increased. This is an important drawback in 2D analysis. At first half of the analysis, the entrainment rate increases to 1.7 m/s rapidly varying between 1 and 2 m/s before the debris stops moving. The maximum height of the rock avalanche decreased with time until the front suddenly reaches the flat area. The calculated maximum height of debris in the deposition area is about 320 m. The calculated maximum entrainment depth is 108 m located at $x = 4{,}218$ m (Fig. 19).

The initial volume of the debris starts at 90×10^6 m³ and increases gradually until the front has moved about 10 km (Fig. 20). When the front has almost stopped, the total volume is still increasing due to the entrainment in the tail region. The maximum increase in volume of 1.03×10^6 m³ occurred at a runout distance of about 5161 m. The front velocity at that location is

higher than 100 m/s. The calculated accumulated volume is not as large as that observed in the field due to neglecting bank entrainment and broadening of flow channel in the entrainment zone.

Validation of modeling results

Validation of the runout and entrainment model is based on field observations such as the estimated runout distance and deposition height. Also, results from published literature are used in evaluating the model. In the model the calculated runout distance is about 10 km which matches the field observation. Since the width of flow channel does not change a lot in entrainment zone, based on the volume of the debris, the depth of entrainment can be calculated. The calculated entrainment depth is the change of the elevation of bed points in the calculation which is adjusted to the direction perpendicular to the slope surface. The observed depth of entrainment versus the calculated values at entrainment zone with a 100-m interval is shown in Fig. 21

To compare the calculated final height of the depositional fan in 2D with field observation which is in 3D, the calculated
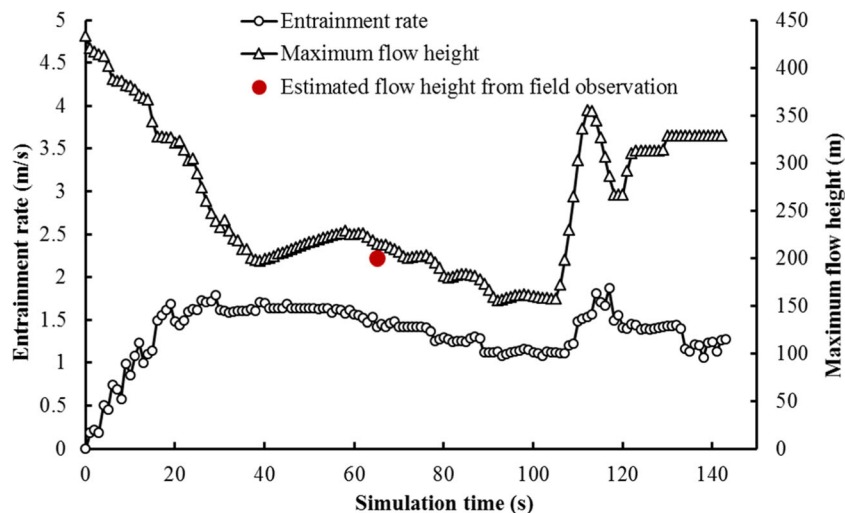

Fig. 18 Maximum entrainment rate and flow height in the simulation of 2000 Yigong rock avalanche
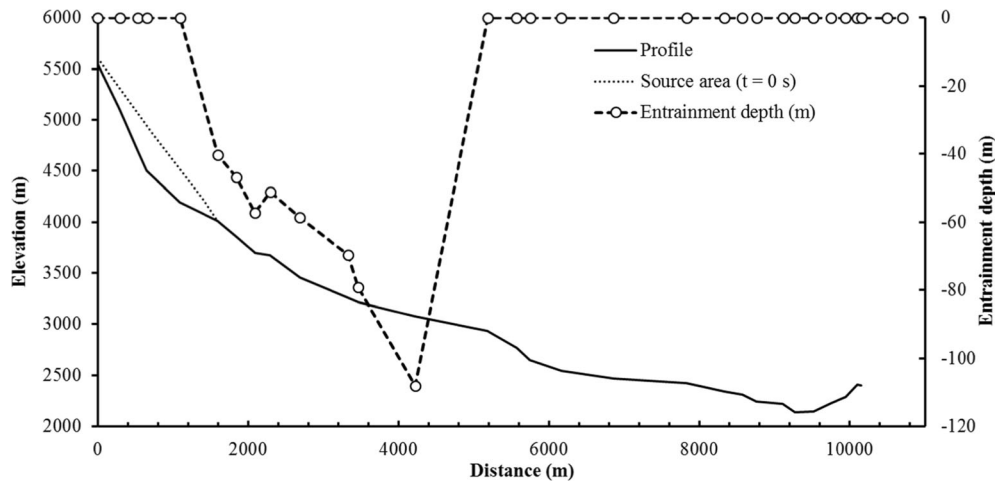
Fig. 19 Calculated entrainment depth along the channel

depositional height has to be adjusted to represent the field situation. A correction coefficient, C_{LS}, for lateral spreading is defined as

$$C_{LS} = W_{model} \Big/ W_{fan} \qquad (7)$$

where W_{model} and W_{fan} are, respectively, the channel width in the model and width of deposition fan. W_{model} is the width of channel calculated by dividing the total volume of source material by total area of source material in 2D profile. W_{fan} is the average width of the deposition fan. A volume and height (h_{fan}) relationship and volume and width (W_{fan}) relationship can be found for this area based on the digital elevation model of deposition fan. Based on this relationship, an equivalent width (W_{model}) can be determined for a rectangular model cross section with the same debris height (h_{fan}) and the same volume. Since the debris flow channel on site is always triangle, the cross section of debris flow channel is changed to rectangle before

calculating W_{fan}. The final deposition height is modified by multiplying the correction coefficient; see Fig. 22. The average flow height measured using a total station is also shown in the figure. It is seen that the modified deposition height is very close to the average value although there are some variations at some points.

YRA is described as a very rapid rock avalanche, but there are very few evidences that can directly provide a measurement of its actual velocity. From the trees destroyed by air pressure wave on two sides of valley and the slurry attached on the trees on the top of a mountain located at left side of the outlet, it can be assumed that YRA occurred with a very high velocity. The calculated maximum velocity is around 110 m/s which agrees reasonably well with the value calculated by Zhang (2013) using DAN 3D. This is a controversial value since this is a very high velocity compared with velocity observed in other cases although description from witness and charred tress along the channel indicated YRA has a very high velocity, but such high peak velocity, 81-100 m/s, has been reported by Evans et al (1989) for case of Pandemonium Creek rock avalanche.
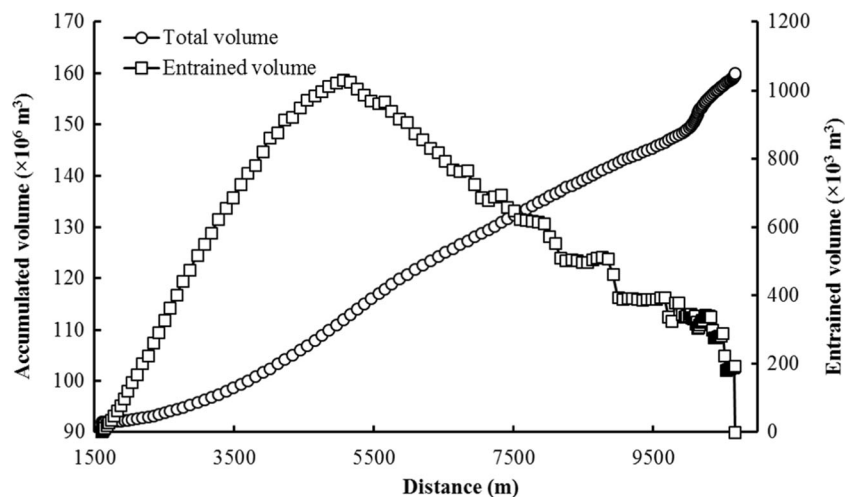

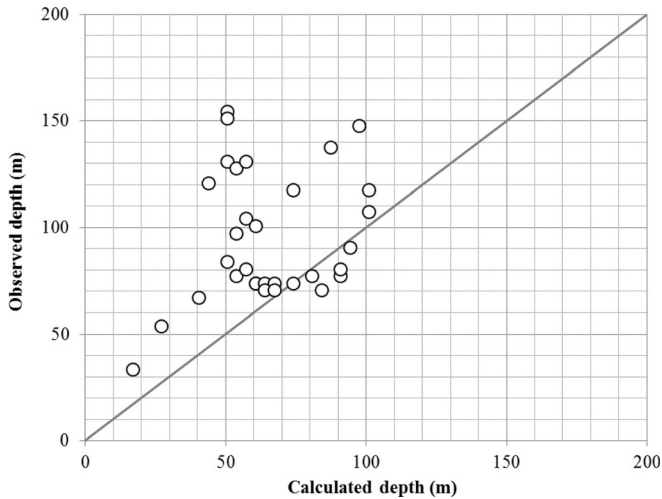**Fig. 20** Entrainment volume and total volume in the simulation

Fig. 21 Comparison between observed entrainment depth in field after event and calculated entrainment depth

To test the effect of entrainment on YRA, the simulation results are compared with and without entrainment; see Fig. 23. It is obvious that the runout distance from the simulation with entrainment is around 1,000 m further than that without entrainment. The front velocity with entrainment is also higher than that without entrainment. This is mainly caused by the increase in potential energy with the introduction of more material in the debris. Moreover, the entrained material will generate more basal friction. The combination of these effects leads to the difference in the runout distance and maximum velocity. Although the differences are not large, since the velocity and runout distance are relatively large due to the scale of the problem, a small increase in velocity and runout distance mean a large increase in kinetic energy. Consequently, the increase in kinetic energy will cause more damages and destructions. The incorporation of entrainment in the debris flow calculation provides a more rational approach than simply assuming a constant volume from start to finish or an empirical assignment of additional mass to the model at specific locations.

At the same time, simulation time for no entrainment is shorter than that with entrainment. It means that omission of entrainment could underestimate the front velocity and runout distance. This could have negative effects in mitigation measures of natural hazards by underestimating the extent and speed of the debris.

Discussion and conclusion

YRA is an extremely large mass movement in recent years. According to the metrological record of weather stations near the Yigong area, rainfall should not be the main trigger of the rock avalanche. Instead, it was found that the most likely triggering mechanism is temperature variation, which resulted in snow/ice melting in cracks and fissures causing the increase in pore water pressure and the decrease in effective stress. Eventually, the slide detached from slope when the shear stress overcomes the shear strength of the rock mass. The YRA occurred at late afternoon when highest GST just pasted few hour ago, this is another evidence that indicates occurrence of YRA is related to the variation of temperature.

It is clearly shown in the simulation results of YRA that the calculated runout distance and flow height at specific locations match reasonably well with the observed value. Also the variation in elevation in the entrainment zone is another indication that the model is reasonable in capturing entrainment. The deposition height of the debris cannot be compared directly with field observation using a 2D model. The height of the debris can cause changes in shear stresses on the channel bed which will change the entrainment rate and depth of erosion. In this model, a lateral spreading correction coefficient is introduced to relate the 2D model with 3D reality. Also the assumption of uniform particle size on the channel bed can increase the discrepancy between calculated results and observed values.

Although the maximum calculated entrainment rate shows some variation with time, the variation is not large except in places where the channel bed is slopping steeply. Entrainment rate of each slice has no regularity along the flow path at different time stage. Entrainment rate in the new model is dependent on slope of flow channel and properties of erodible material. Therefore, estimation of entrainment should be taken those factors into account.
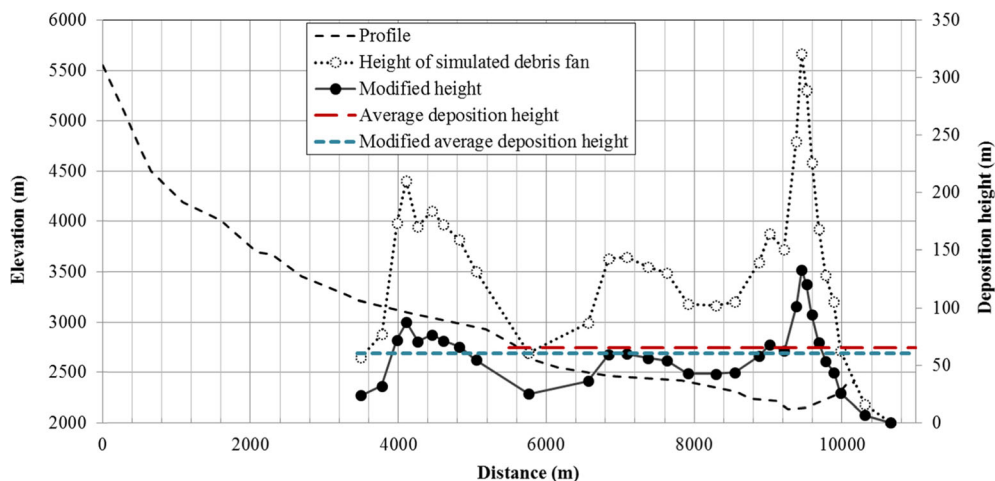

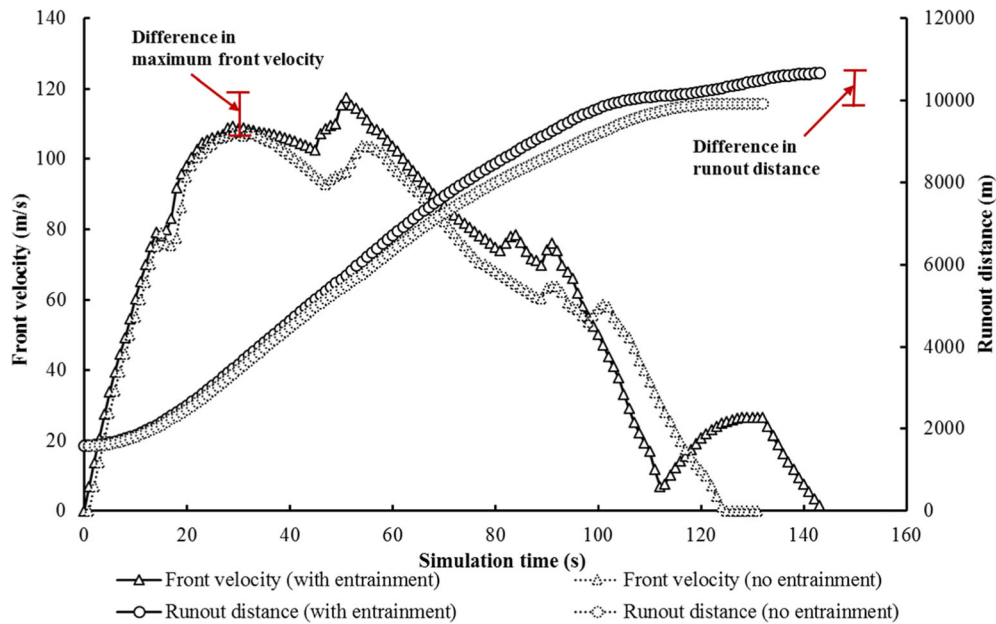**Fig. 22** Modified deposition fan by taking lateral spreading into consideration

Fig. 23 Comparison of maximum velocity and front velocity of YRA with and without entrainment

The proposed entrainment model calculates entrainment volume with time. This is more reasonable in considering progressive scouring since the materials are eroded gradually. Therefore the model can be used to simulate entrainment of channel eroded by flow at different elapsed time. Moreover channel bed elevation is adjusted after each time step to reflect changes due to entrainment which provides a more realistic simulation. This is more important in short channel with a lot of entrainment than a long channel with little entrainment.

Shearing of layers of material refers to the shear failure of material calculated based on static shearing resistance. Instead, the sliding motion refers to the sliding movement of the particle relative to the base material when the low friction is not sufficient to resist motion at the particle contact with the base; otherwise, the rolling motion occurs. This model not only incorporates the rolling motion of entrainment, it also consider the sliding motion of particle and shearing layers of materials which is often the only mechanism considered in many entrainment model. Incorporating the rolling motion in entrainment calculation provides a new concept in advancing the understanding the mechanism of entrainment in debris flow analysis.

One of the uncertainties in the proposed entrainment model is the method in determining the mean value and standard deviation in the PDF. Since the particles in the field are not all spherical in shape and particle size varies a lot, particle protrusion relative to each other is difficult to measure. Therefore particle properties cannot be easy captured using only one PDF. In the case of YRA, the parameters were determined by trial and error based on field observations and empirical relationship.

Reference

Chen XQ (2015) Evidence of flow height near the outlet of Zamu Creek [Fig. 5] (Personal communication, Fig. 5 is proivded by XQ Chen, 11 11 2014)

Chen XQ (2015) Observed largest particle embedded into deposition fan [Fig. 7] (Personal communication, Fig. 7 is proivded by XQ Chen, 11 11 2014)

Cheng NS, Law AWK, Lim SY (2003) Probability distribution of bed particle instability. Adv Water Resour 26(4):427–433

Cundall PA, Strack ODL (1979) A discrete numerical model for granular assemblies. Geotechnique 29:47–65

De Blasio FV, Breien H, Elverhoi A (2011) Modelling a cohesive-frictional debris flow: an experimental, theoretical, and field-based study. Earth Surf Process Landf 36(6):753–766

Egashira S, Honda N, Itoh T (2001) Experimental study on the entrainment of bed material into debris flow. Phys Chem Earth Part C: Solar Terrestrial Planet Sci 26(9):645–650

Evans SG, Clague JJ, Woodsworth GJ, Hungr O (1989) The Pandemonium Creek rock avalanche, British Columbia. Can Geotech J 26(3):427–446

Fannin RJ, Busslinger M, Jordan P (2012) Debris flow travel distance: field traverse data and regional guidelines for terrain stability assessment. Proceedings of the 11th International and 2nd North American Symposium on Landslides. In: Eberhardt E, Froese C, Turner AK, Leroueil S (eds) Banff Canada, June 3-8, 2012, Balkema, Taylor and Francis Group, London, 1: 751-756

Fenton JD, Abbott JE (1977) Initial movement of grains on a stream bed: the effect of relative protrusion. Proceedings of the Royal Society of London Series a—Mathematical Physical and Engineering Sciences 352(1671): 523-537

Fraccarollo L, Capart H (2002) Riemann wave description of erosional dam-break flows. J Fluid Mech 461:183–228

Hungr O (1995) A model for the runout analysis of rapid flow slides, debris flows, and avalanches. Can Geotech J 32(4):610–623

Iverson RM (2012) Elementary theory of bed-sediment entrainment by debris flows and avalanches. J Geophys Res 117:F03006. doi:10.1029/2011JF002189

Li ZL, Komar PD (1986) Laboratory measurements of pivoting angles for applications to selective entrainment of gravel in a current. Sedimentology 33(3):413–423

Liu N, Chen ZL, Cui P, Chen NS (2013) Dammed lake and risk management. Science press, Beijing (In Chinese)

Luna BQ, Remaitre A, van Asch TWJ, Malet JP, van Westen CJ (2012) Analysis of debris flow behavior with a one dimensional run-out model incorporating entrainment. Eng Geol 128:63–75

Lv JT, Wang ZH, Zhou CH (2002) A tentative discussion on the monitoring of the Yigong landslide-blocked lake with satellite remote sensing technique. Acta Geosci Sin 23(4):363–368 (In Chinese)

Medina VH, Bateman A, Hurlimann M (2008a) A 2D finite volume model for bebris flow and its application to events occurred in the Eastern Pyrenees. Int J Sediment Res 23(4):348–360

Medina VH, Hurlimann M, Bateman A (2008b) Application of FLATModel, a 2D finite volume code, to debris flows in the northeastern part of the Iberian Peninsula. Landslides 5(1):127–142

Moffat R, Fannin RJ, Garner SJ (2011) Spatial and temporal progression of internal erosion in cohesionless soil. Can Geotech J 48(3):399–412

Okada Y, Ochiai H (2007) Coupling pore-water pressure with distinct element method and steady state strengths in numerical triaxial compression tests under undrained conditions. Landslides 4(4):357–369

Ren JW, Shan XJ, Shen J, Ge S, Zha S, Deng GY, Zhang J, Suo R (2001) Geological characteristics and kinematics of the rock fall-landslide in Yigong, Southeastern Tibet. Geol Rev 47(6):642–647 (In Chinese)

Schurch P, Densmore AL, Rosser NJ, McArdell BW (2011) Dynamic controls on erosion and deposition on debris-flow fans. Geology 39(9):827–830

Shodja HM, Nezami EG (2003) A micromechanical study of rolling and sliding contacts in assemblies of oval granules. Int J Numer Anal Methods Geomech 27(5):403–424

Skempton AW (1954) The pore-pressure coefficients A and B. Geotechnique 4(4):143–147

Wang ZH (2006) Large scale individual and slide remote sensing. Earth Sci Front 13(5):516–523 (In Chinese)

Wang XB (2008) Geotechnical analysis of flow slides, debris flows, and related phenomena. Dissertation, University of Alberta

Wang ZH, Lv JT (2001) Understand Yigong landslide in Tibet based on the satellite image. J Remote Sens 5(4):312–316 (In Chinese)

Wang XB, Morgenstern N, Chan D (2010) A model for geotechnical analysis of flow slides and debris flows. Can Geotech J 47(12):1401–1414

Xu Q, Shang YJ, Van Asch TWJ, Wang ST, Zhang ZY, Dong XJ (2012) Observations from the large, rapid Yigong rock slide-debris avalanche, southeast Tibet. Can Geotech J 49(5):589–606

Yin YP (2000a) Charateristics and mitigation study on the gigantic Yigong avalanche of Bomi, Tibet, China. Hydrogeol Eng Geol 4:8–11 (In Chinese)

Yin YP (2000b) Introduction on the gigantic Yigong avalanche of Bomi, Tibet, China. Chin J Geol Hazard and Control 11(2):100 (In Chinese)

Zhang YJ (2013) Study on dynamic characteristics of typical rock avalanches on canyon area (Master's thesis). Shanghai Jiaotong University, Shanghai, China (In Chinese)

Zhang M, Yin YP (2013) Dynamics, mobility-controlling factors and transport mechanisms of rapid long-runout rock avalanches in China. Eng Geol 167:37–58

Zhou, GD (2015) Grain size distributions of fine particles (d < 400mm) sampled from runout path of YRA [Fig. 8], (Personal communication, Fig. 8 is proivded by GD Zhou, 04 11 2014)

Zhou GY, Yi YZ (2000) ADCP monitoring in emergency treatment of Yigong massive landslide in Tibet. Yangtze River 31(9):30–32 (In Chinese)

C. Kang (✉) · D. Chan
Department of Civil and Environmental Engineering,
University of Alberta,
Edmonton, Canada
e-mail: ckang3@ualberta.ca

D. Chan
College of Civil Engineering and Architecture,
Three Gorges University,
Yichang, China

F. Su · P. Cui
Institute of Mountain Hazards & Environment,
Chinese Academy of Science,
Chengdu, China